Beam interaction with Plasma-Vacuum interface

(inhomogeneous plasma)

- *Applications to plasma (CLIC breakdown) diagnostics*

Aakash A. Sahai, Thomas C. Katsouleas (Duke University)

aakash.sahai@duke.edu

Random scattering vs

Collective plasma effects

- 30 GeV beam → random scattering
  1 mm water cell
  rms-scattering angle = 20 μ *rad*

- *same* beam → plasma-neutral (vacuum) interface
  10^{-7} *density of water*
  bending angle = 1 *milli rad*

aakash.sahai@duke.edu

Context – High rep-rate Plasma Collider

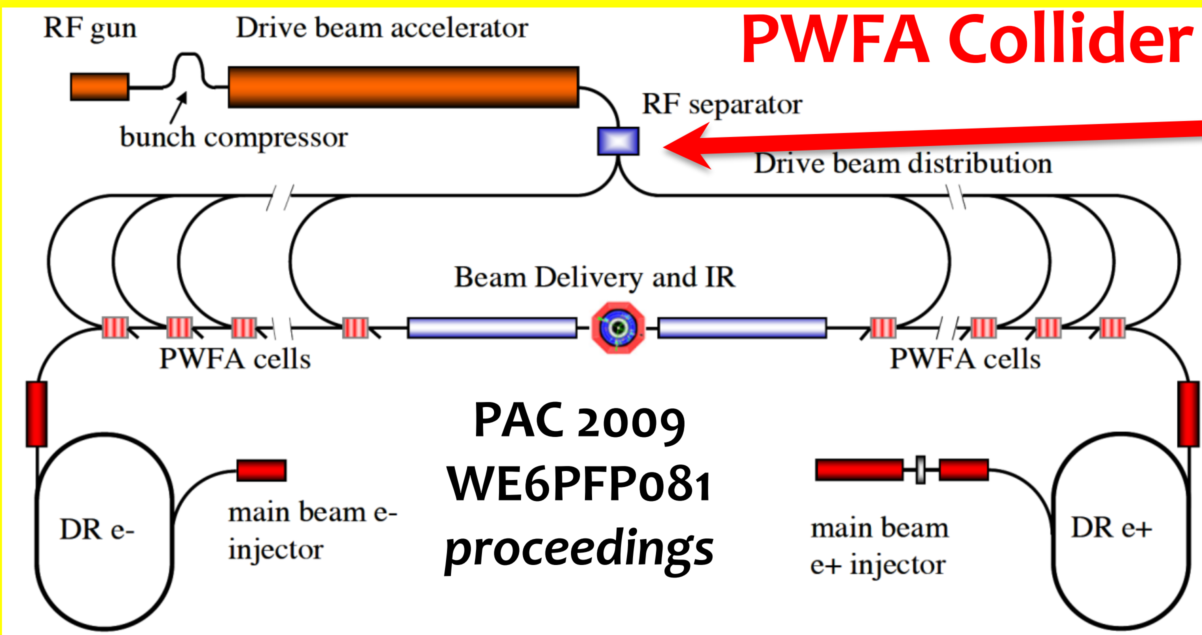

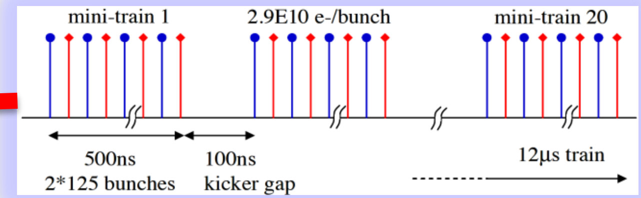

Main beam: bunch population, bunches per train, rate	1×10^{10}, 125, 100 Hz
Total power of two main beams	20 MW
Drive beam: energy, peak current and active pulse length	25 GeV, 2.3 A, 10 μs
Average power of the drive beam	58 MW
Plasma density, accelerating gradient and plasma cell length	1×10^{17} cm^{-3}, 25 GV/m, 1 m
Power transfer efficiency drive beam=>plasma =>main beam	35%
Efficiency: Wall plug=>RF=>drive beam	50% x 90% = 45%
Overall efficiency and wall plug power for acceleration	15.7%, 127 MW
Site power estimate (with 40MW for other subsystems)	170 MW
Main beam emittances, x, y	2, 0.05 mm-mrad
Main beam sizes at Interaction Point, x, y, z	0.14, 0.0032, 10 μm
Luminosity	3.5×10^{34} cm^{-2}s^{-1}
Luminosity in 1% of energy	1.3×10^{34} cm^{-2}s^{-1}

High Luminosity

→ e^- / e^+ bunches per second at IP

CLIC breakdown context - 1

[1] Palaia, A., Farabolini, W., Measurements of the RF breakdown influence on the probe beam, CTF3 working meeting CERN, 11 Oct 2012.

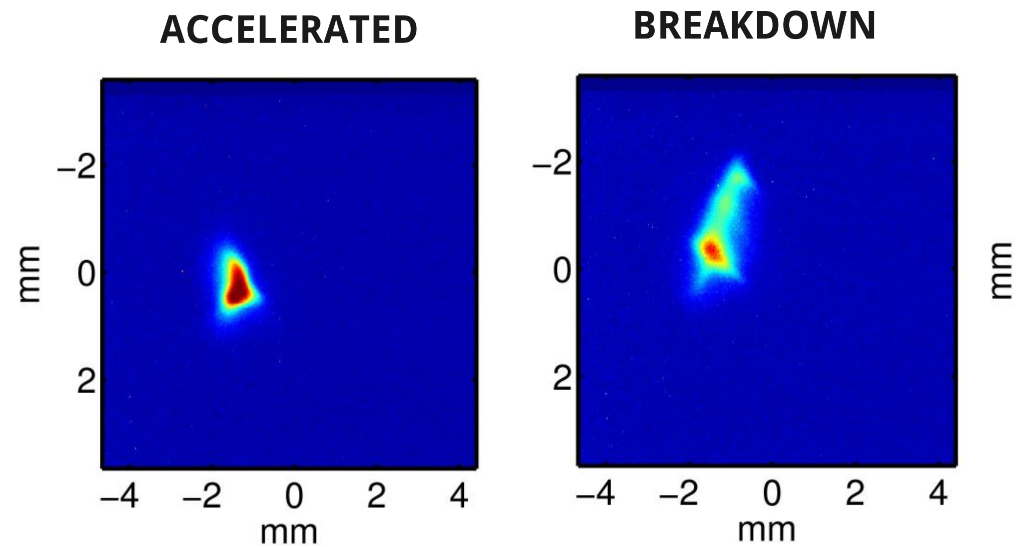

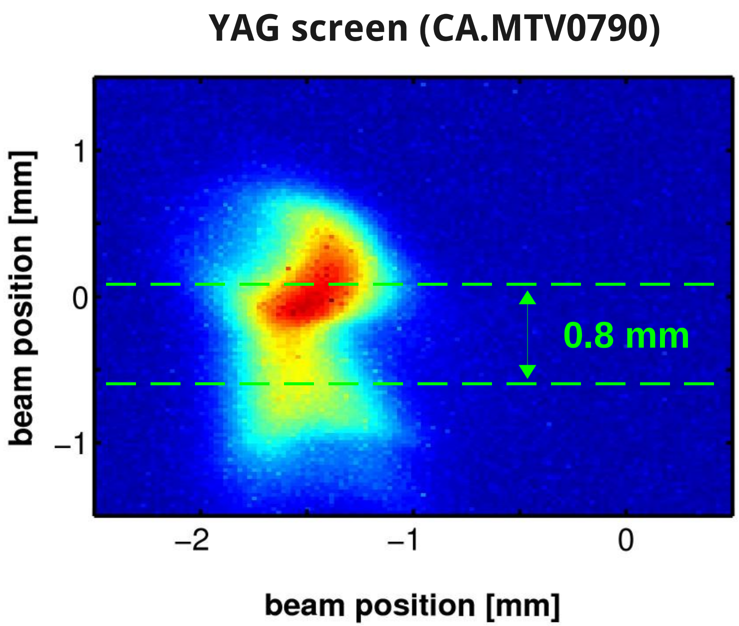

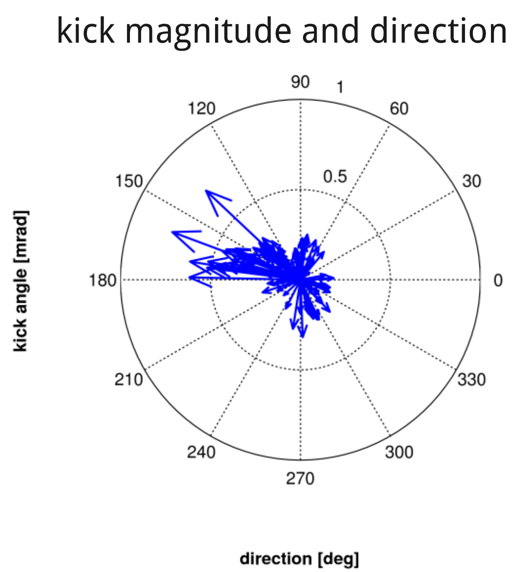

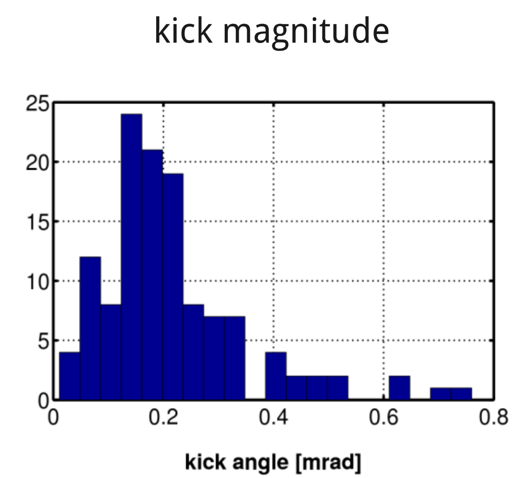

aakash.sahai@duke.edu

CLIC breakdown context - 2

[2] Kovermann, J. W., Stahl, A., Wuensch, W., CERN-THESIS-2010-196 - Aachen: 3. Phys. Inst. RWTH Aachen, 2010.

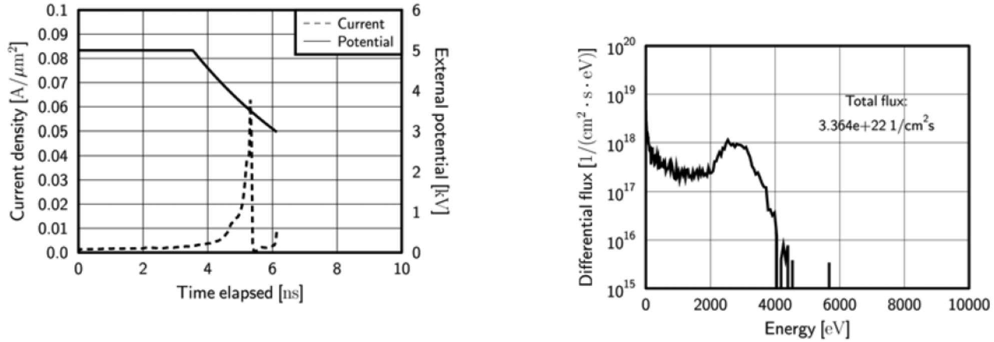

(a) External potential and total current through the discharge gap.

(b) Average Cu^+ energy distribution at the cathode.

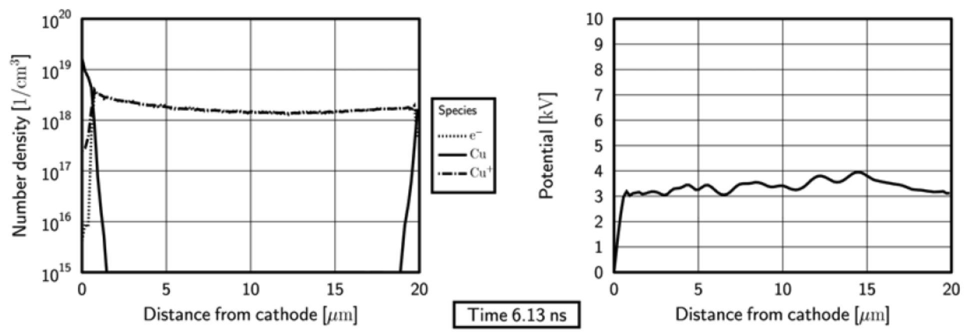

(c) Density of different species (left) and electric potential (right) in the plasma

Fig. 4 Examining the influence of the melting current. The qualitative behaviour remains the same for the whole regime investigated ($j_{melt} = 0.4 - 1$ A/μm^2). In the particular case shown here $\tau = 5$ ns, $r_{Cu/e} = 0.01$ and $j_{melt} = 0.5$ A/μm^2. After the first peak in the total current, a sheath has built up and the total current grows again. (Note that the total current is the sum of the ion and the space charge limited electron current, and stays therefore below j_{melt}.) Fig. (b) shows the average energy distribution of ions bombarding the cathode during the burning of the arc. The densities of different species in the plasma and the corresponding electric potential at the last instant before the simulation exceeds its numerical limits are shown in Fig. (c). Neutrals are present only in the sheath region, while outside the sheath region the plasma is quasi-neutral (electron and ion densities are the same). Quasi-neutrality outside the sheath is reflected also in the constant potential (fluctuations in the potential are due to growing numerical instability at this last instant), whereas the sheath potential originates from the difference in ion and electron densities in the sheath region. Note that also close to the anode there is a sheath potential drop present ($\sim$ 200 eV, corresponding to an electron temperature of $\sim$ 40 eV), however, it is difficult to notice it on the scale of Fig. (c).

aakash.sahai@duke.edu

Expt. 30Gev beam deflection - Boundary effect

[5] Muggli, P., Lee, S., Katsouleas, T., Assmann, R., et al., Boundary effects: Refraction of a particle beam, Nature, **411**, 43, (2001). doi:10.1038/35075144

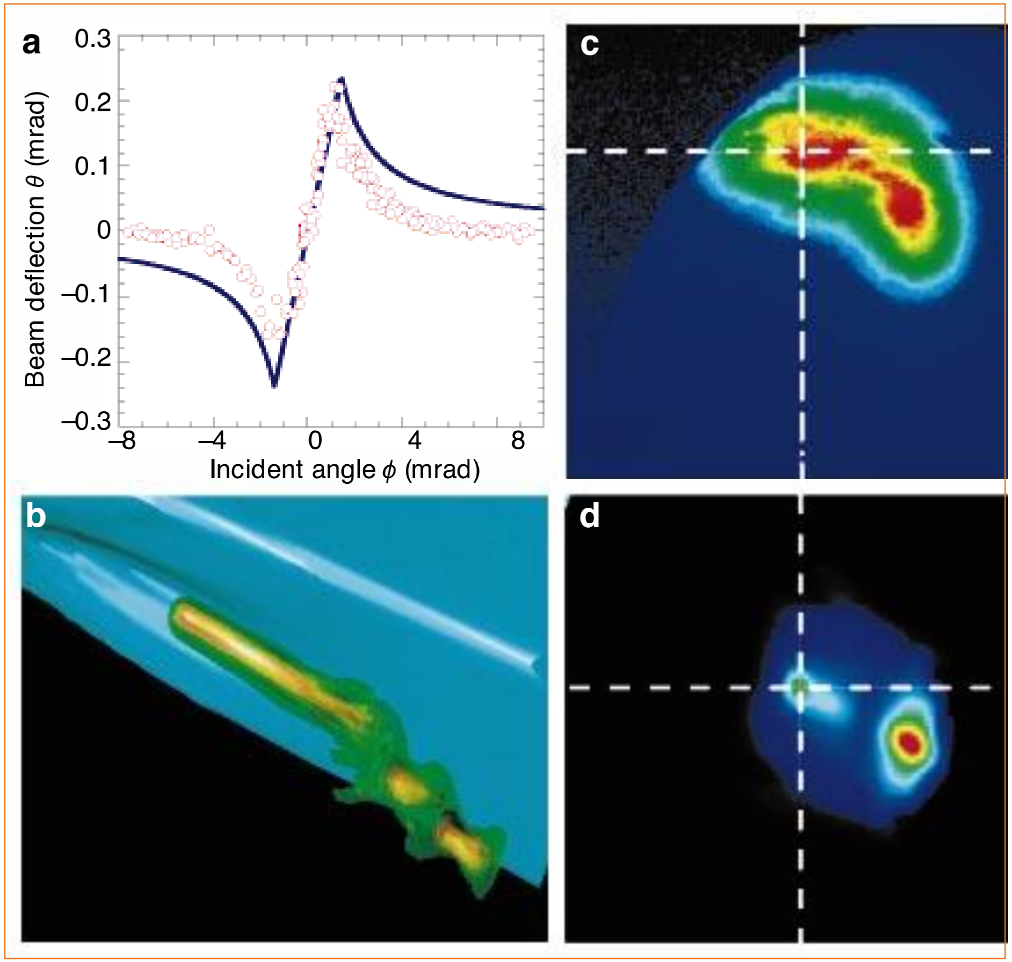

Figure 1 Experimental and simulation results demonstrating refraction of an electron beam at a plasma–gas interface. **a,** Actual electron-beam deflection (circles), measured using a beam-position monitor, and the theoretical deflection (blue line) as a function of the incident angle. **b,** Simulation: perspective image of a beam emerging from plasma (turquoise); the inward motion of the plasma electrons is visible as a depression in the plasma surface behind the beam. **c,** Experiment: image of the beam downstream of the plasma, showing the deflected beam and the undeflected transient (at the crosshairs); **d,** head-on view of image in **b**. The beam consisted of 1.9×10^{10} electrons at 28.5 GeV in a gaussian bunch of length $\sigma_z = 0.7$ mm and spot size $\sigma_x \approx \sigma_y \approx 40$ μm. The plasma, with radius 2.3 mm, length 1.4 m and density 1×10^{14} cm^{-3}, was created by photoionization of lithium vapour by an ArF laser. The angle, ϕ, between the electrons' initial trajectory and the plasma boundary was controlled by adjusting the tilt angle of the final laser-beam mirror.

aakash.sahai@duke.edu

Beam refraction theory - Boundary effect

Denser (Plasma) to Rarer (Neutral) medium → Away from axis

Over-dense beam **→ Ion channel formation** $$\frac{n_b}{n_0} > 1$$

Under-dense beam **→ magnetic pinch force** $$\frac{n_b}{n_0} \leq 1$$

aakash.sahai@duke.edu

Expt. 30Gev beam deflection - boundary theory

Over-dense – beam : $\frac{n_b}{n_0} > 1$

$$\theta_{interface} = \sqrt{8\alpha \frac{N}{\pi\sqrt{2\pi}\sigma_z} \frac{r_e}{\gamma}}$$

formation of Ion-channel !

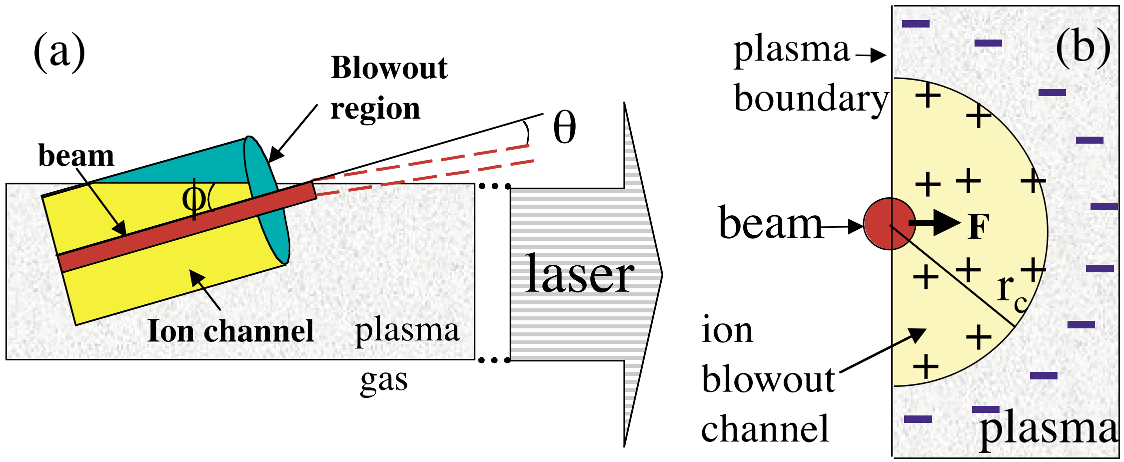

FIG. 1. (Color) Schematic of refraction mechanism. (a) Side view and (b) front view of beam and plasma illustrating how asymmetric blowout creates a net deflection force.

[4] Katsouleas, T., Mori, W. B., Dodd, E., Lee, S., Hemker, R., Clayton, C., Joshi, C., Esarey, E., Laser steering of particle beams: refraction and reflection of particle beams. Nuclear Instruments and Methods in Physics Research A, **455**, 161-165, (2000). doi:10.1016/S0168-9002(00)00724-5

aakash.sahai@duke.edu

30Gev beam deflection – boundary theory

Ion-channel Impulse : $F_{\perp}.\delta t$

Deflection angle : $\frac{p_{\perp}}{p_{||}} = \frac{F.\delta t}{\gamma m_e c}$

Coulomb's Law : $F_{\perp} = -eE = 2n_0 e^2 r_c$

Ion-channel Radius : $r_c = \alpha \sqrt{\frac{n_b}{n_0}} r_b$

Time on boundary : $2\frac{r_c sin\phi}{c}$

Deflection angle : $\theta_{interface} = \frac{1}{sin\phi} 8\alpha \frac{N}{\pi\sqrt{2\pi}\sigma_z} \frac{r_e}{\gamma}$

[6] Muggli, P., Lee, S., Katsouleas, T., et al., Collective refraction of a beam of electrons at a plasma-gas-interface, Physical Review Special Topics - Accelerator and Beams, **4**, 091301 (2001). doi:10.1103/PhysRevSTAB.4.091301

[7] Whittum, D.,Sessler, A., Dawson, J., Ion-Channel Laser, **64**, 21, (1990). 10.1103/Phys-RevLett.64.2511

aakash.sahai@duke.edu

CALIFES beam deflection - theory

$$\phi << 1 rad, \text{ hence } sin\phi \simeq \phi$$

Energy	200 MeV
Energy spread	1% (FWHM)
Pulse length	0.6–150 ns
Bunch frequency	1.5 GHz
Bunch length	1.4 ps
Bunch charge	0.085–0.6 nC
Intensity	
- short pulse	1 A
- long pulse	0.13 A
Repetition rate	0.833 – 5 Hz

$$N = 0.2 \times 10^{10}$$
$$\sigma_z = 1.4\, ps \times c = 0.04\, cm$$
$$\Delta W = 0.15\, cm$$
$$\gamma = 392$$
$$r_e = 2.28 \times 10^{-13}\, cm$$
$$\boxed{r_b = 0.001\, cm} \quad (assumed\ \ 10\mu m)$$

$$\theta_{interface} \text{ of } \boxed{\simeq \ \ 6\, mrad}$$

aakash.sahai@duke.edu

Inhomogeneous plasma beam deflection

Under-dense – beam : $\frac{n_b}{n_0} \leq 1$

No ion channel formation – electron evacuation region !

Ion-channel Impulse : $F_\perp . \delta t$

Deflection angle : $\frac{p_\perp}{p_{||}} = \frac{F.\delta t}{\gamma m_e c}$

Coulomb's Law : $F_\perp = -eE = 2 n_b e^2 r_b$

Edge time: $\Delta t = \frac{W}{c}$

$$\theta = \frac{2 n_b e^2 r_b . \frac{\Delta W}{c}}{\gamma m_e c}$$

$$= 2 \left(\frac{N}{\sqrt{2\pi}\, \sigma_z \pi r_b^2} \right) r_b \frac{e^2}{\gamma m_e c} \left(\frac{\Delta W}{c} \right)$$

$$= 2 \frac{N}{\pi \sqrt{2\pi}\, \sigma_z} \frac{e^2 / m_e c^2}{r_b} \frac{\Delta W}{\gamma}$$

$$\boxed{\theta_{inhomogeneous} = 2 \frac{N}{\pi \sqrt{2\pi}\, \sigma_z} \frac{r_e}{r_b} \frac{\Delta W}{\gamma}}$$

$$\theta_{inhomogeneous}$$

$$\boxed{\simeq \quad 137\ mrad}$$

aakash.sahai@duke.edu

Thank You !

aakash.sahai@duke.edu